Control of 2D plasmon-polariton mode with dielectric nanolayers

Junpeng Guo and Ronen Adato

Department of Electrical and Computer Engineering
University of Alabama in Huntsville, Huntsville, AL 35899
jguo@eng.uah.edu

Abstract: We introduce two nanoscale thickness dielectric layers on the top and bottom sides of a finite width and finite thickness metal microstrip and have calculated the fundamental symmetric plasmon-polariton mode of the 2D metal-dielectric layer waveguide. The dielectric nanolayers provide an additional degree of freedom to control the plasmon-polariton mode. When the dielectric constant of the nanolayers is smaller than that of the cladding dielectric, the travel range of the fundamental symmetric plasmon-polariton mode is extended with the trade-off of the mode confinement. The figure of merit of the mode increases as the travel range extends.

OCIS codes: (240.6680) Surface plasmons; (130.2790) Guided waves

References and links

1. E. A. Stern and R. A. Ferrell, "Surface plasma oscillations of a degenerate electron gas," Phys. Rev. **120**, 130-136 (1960).
2. H. Raether, *Surface Plasmons on Smooth and Rough Surfaces and on Gratings* (Springer-Verlag, Berlin, 1988).
3. E. N. Economou, "Surface plasmon in thin films," Phys. Rev.**182**, 539-554 (1969).
4. D. Sarid, "Long-range surface-plasma waves on very thin metal films," Phys. Rev. Lett. **47**, 1927-1930 (1981).
5. G. I. Stegeman, J. J. Burke, and D. G. Hall, "Surface-polariton like waves guided by thin, lossy metal films," Opt. Lett. **8**, 383-386 (1983).
6. F. Yang, J. R. Sambles, and G. W. Bradberry, "Long-range surface modes supported by thin films," Phys. Rev. B **44**, 5855 (1991).
7. P. Berini," Plasmon polariton modes guided by a metal film of finite width," Opt. Lett. **24**, 1011-1013 (1999).
8. P. Berini, "Plasmon polariton waves guided by thin lossy metal films of finite width: bound modes of symmetric structures," Phys. Rev. B **61**, 10484-10503 (2000).
9. B. Lamprecht, J. R. Krenn, G. Schider, H. Ditlbacher, M. Salerno, N. Felidj, A. Leitner, F. R. Aussenegg, and J. C. Weeber, "Surface plasmon propagation in microscale metal stripes," Appl. Phys. Lett. **79**, 51-53 (2001).
10. R. Zia, A. Chandran, and M. L. Brongersm, "Dielectric waveguide model for guided surface polaritons," Opt. Lett. **30**, 473-1475 (2005).
11. A. Degiron and D. Smith," Numerical simulations of long-range plasmons," Opt. Express **14**, 1611-1625 (2006).
12. P. Berini, "Long-range surface plasmon-polariton waveguides in silica," J. Appl. Phys. **102**, 053105 (2007).
13. S. J. Al-Bader, "Optical transmission on metallic wires-fundamental modes," IEEE J. Quantum Electron. **40**, 325-329 (2004).
14. A. E. Craig, G. A. Olson, and D. Sarid, "Experimental observation of the long-range surface-plasmon polariton," Opt. Lett. **8**, 380-382 (1983).
15. R. Charbonneau, P. Berini, E. Berolo, and E. Lisicka-Shrzek, "Experimental observation of plasmon polariton waves supported by a thin metal film of finite width," Opt. Lett. **25**, 844-846 (2000).
16. R. Charbonneau, N. Lahoud, G. Mattiussi, and P. Berini, "Demonstration of integrated optics elements based on long-ranging surface plasmon polaritons," Opt. Express **13**, 977-984 (2005).
17. T. Nikolajsen, K. Leosson and S. I. Bozhevolnyi, "In-line extinction modulator based on long-range surface plasmon polaritons," Opt. Commun. **244**, 455-459 (2005).
18. Y. Wang, R. Islam, and G. V. Eleftheriades, "An ultra-short contra-directional coupler utilizing surface plasmon-polaritons at optical frequencies," Opt. Express **14**, 7279-7290 (2006)
19. L. Wendler and R. Haupt, "Long-range surface plasmon-polaritons in asymmetric layer structures," J. Appl. Phys. **59**, 3289-3291 (1986).
20. F. Y. Kou and T. Tamir, "Range extension of surface plasmons by dielectric layers," Opt. Lett. **12**, 367-369 (1987).

#90484 - $15.00 USD Received 4 Dec 2007; revised 14 Jan 2008; accepted 14 Jan 2008; published 16 Jan 2008

21. N. M. Lyndin, I. F. Salakhutdinov, V. A. Sychugov, B. A. Usievich, F. A. Pudonin and O. Parriaux, "Long-range surface plasmons in asymmetric layered metal-dielectric structures," Sens. Actuators B **54**, 37-42 (1999).
22. J. Guo and R. Adato, "Extended long range plasmon waves in finite thickness metal film and layered dielectric materials," Opt. Express **14**, 12409-12418 (2006).
23. R. Adato and J. Guo, "Characteristics of ultra-long range surface plasmon waves at optical frequencies," Opt. Express **15**, 5008-5017 (2007).
24. P. B. Johnson and R. W. Christy, "Optical constants of the noble metals," Phys. Rev. B **6**, 4370-4379 (1972).
25. FIMWAVE Version 4.5 Reference Manual 2006, Photon Design Ltd, Oxford, United Kingdom.
26. A. S. Sudbo, "Film mode matching: a versatile numerical method for vector mode field calculations in dielectric waveguides," Pure Appl. Opt. **2**, 211-233 (1993).
27. P. Berini, "Figures of merit for surface plasmon waveguides," Opt. Express **14**, 13030-13042 (2006).
28. Robin Buckley and Pierre Berini, "Figures of merit for 2D surface plasmon waveguides and application to metal stripes," Opt. Express **15**, 12174-12182 (2007).
29. R. Zia, M. D. Selker, P. B. Catrysse, and M. L. Brongersma, "Geometries and materials for subwavelength surface plasmon modes," J. Opt. Soc. Am. A **21**, 2442-2446 (2004).
30. G. I. Stegeman and J. J. Burke, "Effects of gaps on long range surface plasmon polaritons," J. Appl. Phys. **54**, 4841-4843 (1983).
31. Pierre Berini, "Air gaps in metal stripe waveguides supporting long-range surface plasmon polaritons," J. Appl. Phys. **102**, 033112 (2007).
32. Z. Sun, "Vertical dielectric-sandwiched thin metal layer for compact, low-loss long range surface plasmon waveguiding," Appl. Phys. Lett. **91**, 111112 (2007).
33. P. Berini, R. Charbonneau, and N. Lahoud, "Long-range surface plasmons on ultrathin membranes," Nano Lett. **7**, 1376-1380 (2007).

1. Introduction

Surface plasmons are free electron density oscillations on the surface of metals in dielectric materials [1, 2]. The propagation of a surface plasmon is always coupled with a surface electromagnetic wave along the metal-dielectric boundary. The coupled physical state between the surface plasmon and the electromagnetic wave is called the surface plasmon-polariton (SPP). Although surface plasmon-polaritons can propagate along surfaces of metals, a fundamental problem of surface plasmon-polaritons is the large attenuation due to the intrinsic free electron collision loss inside the metal.

Significant efforts have been made in the past several decades to extend the travel range of surface plasmon-polaritons. Using thin metal films as low loss plasmon guides was first proposed in 1969 [3]. For a thin metal film of thickness thinner than the surface plasmon penetration depth in the metal, the surface plasmon waves along the two surfaces are coupled together [4-6]. Finally, at least two guided plasmon modes are supported. One plasmon mode has the symmetric magnetic field mode profile with respect to the center of the metal film. Another plasmon mode has the anti-symmetric magnetic field mode profile with respect to the center of the metal film. The travel range of the symmetric plasmon mode is longer than the travel range of the surface plasmon along the single surface of the bulk metal. It is also called the long range surface plasmon-polariton (LRSP) mode. The anti-symmetric mode has higher attenuation and is also called the short range surface plasmon-polariton mode.

Thin metal film plasmon waveguides have limited applications due to the lack of lateral confinement. Surface plasmon-polaritons can also be guided by finite width metal strips [7-12] and metal nanowires [13]. A metal strip or nanowire in a homogeneous dielectric medium typically supports multiple bound plasmon modes depending on the cross section and the materials of the waveguide. Among the multiple modes, there always exists one symmetric plasmon mode. The dominant magnetic field component and the power density profiles are symmetric in both x and y directions for the symmetric plasmon mode. This symmetric plasmon mode is of most interest since it has longest travel range among the modes supported by the same structure. Plasmon waveguides and functional plasmon waveguide devices have been experimentally demonstrated by many groups [14-18].

Range extension of plasmon waves along finite thickness metal films was studied by locating the thin metal film between two semi-infinite homogeneous different dielectric materials [19]. By properly choosing the dielectric materials on each side, a significant portion

#90484 - $15.00 USD Received 4 Dec 2007; revised 14 Jan 2008; accepted 14 Jan 2008; published 16 Jan 2008

of the SPP energy propagates in the high dielectric medium in one side, and a small portion of the SPP energy propagates in the metal layer. Range extension of plasmon waves was also investigated by coupling a plasmon metal waveguide with a dielectric waveguide. By properly designing the coupled waveguide, most energy propagates in the dielectric layers and less energy propagates in the metal layer [20]. Therefore, the travel range wave can be extended. The extended long range mode was a leaky mode in [20]. Metal-dielectric layer asymmetric plasmon waveguides were previously investigated and reported [21].

Recently, we reported that by placing thin dielectric layers of a lower dielectric constant than that of the cladding on both surfaces of a thin metal film, the travel range of the 1D fundamental symmetric plasmon mode can be significantly extended [22, 23]. Because 1D plasmon waveguides lack the lateral confinement, their applications are very limited. In this paper, we report our investigation of the mode properties of a finite width metal strip with lower dielectric constant nanolayers on the both sides. In addition to show the range extension effect as in the 1D plasmon waveguide, we also report our investigation of the effect on the figure of merit of the 2D plasmon waveguide. The 2D metal-dielectric layer plasmon waveguide can be easily fabricated with the standard photolithography fabrication process and have significant impact in building low-loss plasmon circuits for many applications.

2. Finite width metal strip plasmon waveguide with dielectric nanolayers

Figure 1 shows the cross section of a metal strip plasmon waveguide with hetero-dielectric nanolayers. The metal strip has a width of *w* in the *x* direction and a thickness of *t* in the *y* direction. The propagation of the SPP is in the z direction (normal to the x and y directions). We place two identical thin dielectric layers of lower dielectric constant than that of cladding dielectric on top and bottom sides next to the metal layer. The dielectric nanolayers have the same width as the finite width metal strip (*w*) and each of them has a thickness of *d*. The thickness (*d*) of the dielectric nanolayers is smaller than the plasmon field penetration depth outside of the metal layer. The metal-dielectric layer structure forms the core of the plasmon waveguide and is embedded in a higher dielectric constant dielectric material. The plasmon waveguide structure is symmetric in both x and y directions. Since the dielectric layers have lower index of refraction than that of the cladding dielectric, all the guided modes, if exist, are due to the plasmonic effect.

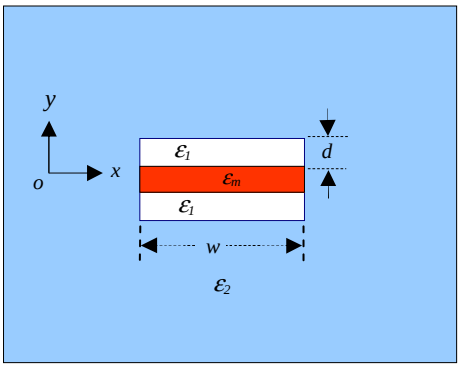

Fig. 1. The cross section of the finite width metal strip plasmon waveguide with dielectric nanolayers. The metal strip (red in the center) is sandwiched between two dielectric nanolayers of dielectric constant (ε_1) less than that of the dielectric cladding (ε_2).

The relative electric permittivity of metal strip (red in the center) is ε_m. Two dielectric nanolayers have the dielectric constant of ε_1. The metal and dielectric nanolayers are embedded in a homogeneous dielectric cladding of larger dielectric constant (ε_2) than the dielectric nanolayers ($\varepsilon_1<\varepsilon_2$). The metal strip is a gold (Au) strip of 1μm wide in the *x* direction and 20 nm thick in the *y* direction. The nanolayers are chosen to have dielectric constant of $\varepsilon_1= (1.45)^2$. The cladding dielectric is chosen to have the dielectric constant of $\varepsilon_2=$

#90484 - $15.00 USD Received 4 Dec 2007; revised 14 Jan 2008; accepted 14 Jan 2008; published 16 Jan 2008

$(1.6)^2$. In our calculations, the plasmon frequency corresponds to the wavelength of $\lambda = 850\,\text{nm}$ in the vacuum. The relative electric permittivity of the gold film at this frequency is $\varepsilon_m = -28.28 - j1.557$ from the measurement of Johnson and Christy [24].

3. The calculation results

The plasmon-polariton modes supported by the metal-dielectric structure in Fig. 1 can be obtained by solving the Maxwell's equations with the boundary conditions. We calculated the mode index and the electromagnetic mode profiles by using a commercial code FIMMWAVE [25], which is a fully vectorial mode solver based on the film mode matching (FMM) method [26]. The essential idea of the FMM method is dividing the waveguide structure into multiple slices in the x-direction so that each slice does not vary with the x. In the each slice, the complete set of one-D modes forms a base such that any field can be written as a linear combination of these modes. In the calculation, the number of one-D modes needs to be truncated, but it still provides a good approximation if the number of one-D modes is large. After the one-D modes are found, boundary conditions are applied at all the boundaries of slices. In order to get the one-D modes, the top and bottom boundary conditions have to be set. We choose the impedance boundary condition for the top and the bottom boundaries. The boundary impedances are ratios of tangential component of electric field to the tangential component of the magnetic field ($Z = E_z/H_x = -E_x/H_z$) [25]. For the nanolayer thickness from 0 to 31.5 nm, the calculation domain is 200 micron by 200 micron, the number of one-D modes in each slice is 180, and the boundary impedance is $0.15j$ Ohm. For the nanolayer thickness from 32 to 35 nm, the calculation domain is 500 micron by 500 micron, the number of one-D modes in each slice is 360, and the boundary impedance is $0.094j$ Ohm. The criteria for choosing the value of the boundary impedance is that the mode profiles are not effected by the presence of boundaries. The left and right boundaries of the calculation window are transparent boundaries which mean that same material extends to infinite and the electromagnetic field approaches to zero at the infinite.

Since the structure is invariant in the z-direction and the modes are propagating in the z-direction, the z-dependence of the electromagnetic wave is described by $\exp[-j\frac{2\pi}{\lambda}n_{eff}z]$, where $n_{eff} = n - jk$ is the mode index. The imaginary part (k) of the mode index determines the travel range ($L_s = \lambda/4\pi k$). Figure 2 shows the calculated real part (solid red line) and the imaginary part (dashed blue line) of the mode index versus the nanolayer thickness. As the nanolayer thickness is increased, the waveguide supports lower attenuation and thus longer range plasmon mode.

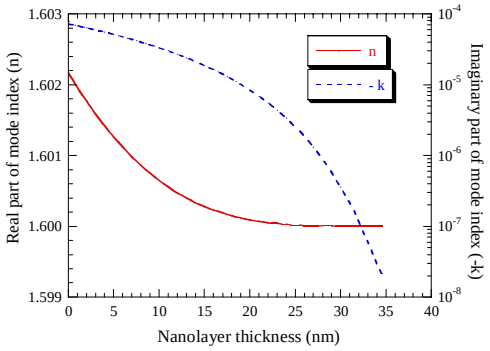

Fig. 2. The real part (sold line) and imaginary part (dashed line) of the mode index versus the nanolayer thickness.

The travel range versus nanolayer thickness is shown as the blue curve in the Fig. 3. As the nanolayer thickness increases from 0 to 30 nm, the travel range increases from 935 micron to 19 cm. Further increasing the nanolayer thickness, the travel range can be further increased. The travel range approaches to infinite as the nanolayer thickness approaches to a critical

#90484 - $15.00 USD Received 4 Dec 2007; revised 14 Jan 2008; accepted 14 Jan 2008; published 16 Jan 2008

thickness. At the critical thickness, the mode becomes cut-off. At the cut-off, the mode size is infinite large. We use one of the figures of merits proposed in [27, 28] to characterize the mode. The figure of merit is the ratio of the travel range to the effective mode size of the 2D plasmon mode. The effective mode size (s) is the diameter of a circle which has the same area of the plasmon mode. The mode area is calculated from the mode spatial extent in x direction (s_x) and the mode spatial extent in the y direction (s_y). To follow the convention, the mode spatial extent is defined as the full 1/e width of the electromagnetic field on the cross section of the waveguide. The figure of merit is plotted as the dashed red line curve in the Fig. 3. The figure of merit increases as the nanolayer thickness increases. This indicates that the travel range increases faster than the mode size increases.

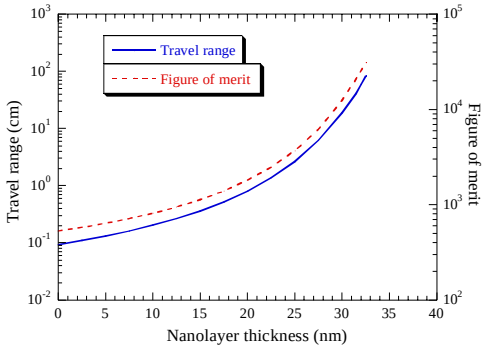

Fig. 3. The travel range and the figure of merit versus the thickness of nanolayers.

The power density profile is the Poynting vector component in the z direction. Figure 4 (a)-4(c) show the 2D power density plots of the plasmon modes for nanolayer thicknesses of d = 0, 10, 20 nm. The power density inside the metal is negative and has a small value. At d = 0, the finite width metal strip plasmon waveguide does not have dielectric nanolayers. This structure has been extensively investigated [7-11]. As the nanolayers are introduced and the thickness increases, the mode size increases. Figure 4(d) shows the plots of the spatial extents of the mode in the x and y directions versus the nanolayer thickness. Large mode size indicates that a large portion of the plasmon-polariton energy propagates outside the metal layer. The ultra-long travel range showed in Fig. 3 can be explained by the mode size expansion caused by the low dielectric constant nanolayers next to the metal layer. This is consistent with the trade-off between the attenuation and the mode confinement discussed in [27-29]. A large size plasmon mode has less portion of surface plasmon-polariton energy inside the metal layer, therefore longer travel range. The dielectric nanolayers introduced here provide a control to the plasmon mode properties. Figure 4(d) also shows that there is a large range of nanolayer thickness (d) to control the plasmon mode properties.

Effects of air gaps on the long range plasmon mode of the metal slab waveguide were studied long time ago [30]. The effects of the air gap were found to be deleterious because they cause the long-range modes to be cut off for very small air gaps. After we finished our calculations, we noticed that the effects of various air gap configurations along finite width metal strips were carefully studied and recently reported in [31]. In general, plasmon modes are very sensitive to the air gaps. Although air gaps can reduce the attenuation and the confinement of the plasmon modes, they push the plasmon modes to become cut-off quickly. This makes the air gaps deleterious for practical applications. That air gaps push the plasmon modes to become cut-off quickly is due to the large index contrast between the air gaps and the cladding dielectric. The real part of the mode index is quickly reduced to the index of refraction of the cladding by the air gaps. In our plasmon waveguide, the index contrast between the cladding and the nanolayers is small. Therefore it can support symmetric plasmon mode which is far away from the cut-off. The attenuation and mode size can be designed to meet practical applications. For example, the mode without nanolayers has a mode size of

#90484 - $15.00 USD Received 4 Dec 2007; revised 14 Jan 2008; accepted 14 Jan 2008; published 16 Jan 2008

about 1.76 micron and a travel range of 935 micron. With the nanolayers of thickness d = 25 nm, the travel range extends to 2.65 cm and the mode size is 7.18 micron. The travel range increases a factor of 28, which is one of magnitude longer than the plasmon range without nanolayers while it still keeps the mode size of the order of microns.

In this paper, we calculate the effects of lower dielectric constant nanolayers on the fundamental symmetric plasmon mode of a finite width metal strip guide. In contrast to the lower dielectric constant nanolayers, higher dielectric constant nanolayers will enhance the mode confinement and reduce the travel range. By reducing the mode size with higher index dielectric nanolayers, the radiation bending loss of plasmon waveguide can be reduced [32]. Because of the tight energy confinement with higher index nanolayers, surface electromagnetic fields near the metal layer can be enhanced. More sensitive biosensors can be realized with nanolayer enhanced surface electromagnetic fields [33].

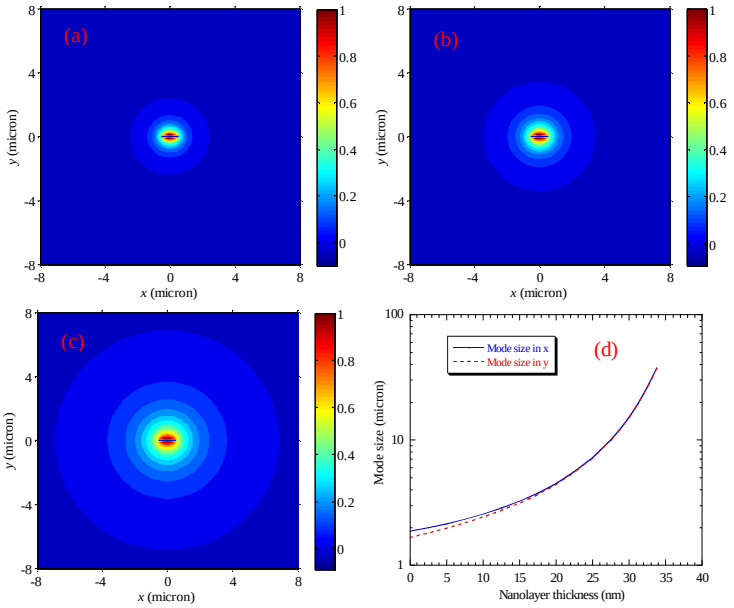

Fig. 4. The 2D power intensity plots of the symmetric plasmon modes without nanolayers (a) d= 0 nm and with nanolayers of thickness (b) d =10 nm and (c) d=20 nm; the (d) shows the mode spatial extents in the x and y directions versus the nanolayer thickness.

4. Summary

We investigated a 2D plasmon waveguide structure which has an additional degree of freedom to control the mode properties of the symmetric plasmon-polariton mode along a finite width metal strip of finite thickness. In the 2D plasmon waveguide, we introduce two dielectric nanolayers on the two sides of the metal layer. The dielectric nanolayers have a different dielectric constant from that of the cladding dielectric. Since the surface plasmon-polariton energy is localized near the surfaces of the finite width metal strip, the mode properties are sensitive to the dielectric nanolayers. We investigated the effect of the dielectric nanolayers on the attenuation and the mode size of the fundamental symmetric plasmon mode. We found that the lower dielectric constant nanolayers extend the travel range with the cost of the increased mode size. When the thickness of the dielectric nanolayers increases, the travel range increases faster than the mode size increases.

#90484 - $15.00 USD Received 4 Dec 2007; revised 14 Jan 2008; accepted 14 Jan 2008; published 16 Jan 2008